



Good performance of low-cost carbon dioxide sensor based on intercomparisons with the standard eddy-covariance system

Üllar Rannik¹, Ivan Mammarella¹, Timo Vesala¹, Pirkko Väkimies², Hilikka Heiskari-Tuohiniemi², Mika Korkiakoski³

5 ¹Institute for Atmospheric and Earth System Research/Physics, University of Helsinki, Finland

²Vaisala Oyj, Vantaa, Finland

³Finnish Meteorological Institute, Helsinki, Finland

Correspondence to: Üllar Rannik (ullar.rannik@heuristic.ae)

Abstract. Flux measurements have started to play an important role outside academia in assessing carbon sinks of different ecosystems and land-use types. If natural carbon solutions are to be deployed and monetized in carbon markets, more low-powered and low-cost flux systems should be deployed. There is a growing need for low-cost sensors that still fulfil the requirements for scientific applications. We present a case study where Vaisala company and the University of Helsinki joined their industrial and academic competencies to create an inexpensive yet precise fast-response carbon dioxide (CO₂) and water vapour (H₂O) sensor. A working prototype was developed and field-tested against a scientific reference eddy covariance (EC) setup. Special attention was paid to response time, lowered sampling frequency, and auto-calibration related to the temperature. The results at the end of the project were very promising. The enclosed-path EC prototype had a CO₂ response time of 0.18 sec and a noise level of 1 ppm at a 5 Hz sampling rate. The internal auto-calibration procedure was continuously improved such that CO₂ signal drifting was avoided and the instrument was capable of measuring CO₂ fluxes with high correlation relative to the reference EC setup ($R^2 = 0.98$).

20 1 Introduction

Multiple initiatives, such as Land Use, Land-Use Change and Forestry (LULUCF) activities, promote EU countries to reduce their greenhouse gas (GHG) emissions (e.g. Romppanen, 2020). There has been discussion of forming carbon (C) markets where countries and companies can trade C credits depending on their GHG emission needs. For example, in agriculture, interest in carbon farming has increased, where the aim is to store C in soil. Soil C content can be measured using inventory-based methods, but those are difficult to apply in practice and do not provide results within short time periods (5-10 years). The alternative method is eddy covariance (EC), which allows measurement of fluxes on 30 min timescale. However, the method utilizes relatively expensive instrumentation. If the price of instrumentation could be reduced, the technique would become more accessible (e.g. Baldocchi, 2019). Low-cost (LC) instrumentation would also enable increasing the number of measurement locations across heterogeneous ecosystems, or adding several EC setups at the same site would improve the confidence of the carbon balance at an annual scale (Hill et al., 2017).

Several studies have utilized an LC EC setup to measure water vapour (H₂O) fluxes, achieving good agreement with a reference setup. Markwitz and Siebicke (2019) performed a case study of evapotranspiration measurements over agroforestry and conventional agricultural sites using the LC relative humidity sensor. The thermohygrometer (BME280 manufactured by Robert Bosch GmbH, Stuttgart, Germany) used in the LC setup had a response time of 1 sec. The authors compared the measurements obtained with the LC setup with the conventional EC setup and reported good correspondence of results within the range of 14% flux underestimation to 8% overestimation. In addition, Wang et al. (2024) utilised a cost-efficient open-path H₂O analyzer (model HT1800, HealthyPhoton Technology Co., China) based on the tunable diode laser absorption spectroscopy technique. The field performance of the two LC analyzers operating at different wavelengths (1392 nm and 1877



40 nm) was evaluated through inter-comparative experiments with LI-7500RS (Li-Cor Environmental, Lincoln, NE, USA) and
IRGASON (Campbell Scientific, Inc., USA), two of the most used H₂O analyzers in the EC community. In spite of all
instruments experiencing drift relative to the reference sensor (low-drift temperature and humidity probe; model HMP155,
Vaisala, Helsinki, Finland), the half-hourly H₂O fluxes measured by HT1800 were highly consistent with those by LI-7500RS
and IRGASON (with a difference of less than 2%). Wang et al. (2024) concluded that HT1800 can obtain H₂O fluxes with
45 high confidence and proved to be suitable for EC application in terms of data availability, flux detection limit and response to
the high-frequency turbulent variation.

Compared to LC EC H₂O flux measurements, the results from LC EC CO₂ flux studies have been more variable, but still
promising. Hill et al. (2017) utilised multiple Vaisala GMP343 CO₂ sensors (Vaisala Oyj, Helsinki, Finland) together with
50 Honeywell HIH-4000 (Honeywell International Inc., Charlotte, North Carolina, USA) relative humidity sensor at the same site
to increase the statistical confidence of the annual flux at the ecosystem level. The selected CO₂ sensors with a 0-2000 ppm
range had a quoted accuracy of ± 5 ppm +2% of the reading and a frequency response equivalence of 0.74 Hz. Cunliffe et al.
(2022) deployed eight LC EC systems in two clusters around two conventional EC systems in the Chihuahuan Desert of North
America for two years. The sites were characterized by large temperature variations and relatively low CO₂ fluxes represented
55 a challenging setting for EC. The LC systems utilized a Vaisala GMP343 sensor for CO₂ and a Honeywell HIH-4000 sensor
for relative humidity. The authors found very good correspondence between the LC and conventional systems' fluxes of latent
energy (evapotranspiration; with a concordance correlation coefficient ≥ 0.89), and promising correspondence in the net
ecosystem exchange (NEE) with a respective correlation coefficient ≥ 0.4 at the daily temporal resolution. Relative to the
conventional systems, the LC systems were characterized by a higher level of random error, particularly in the NEE fluxes.

60 Ramshorst et al. (2024) tested the performance of an LC EC setup for CO₂ and H₂O flux measurements at an agroforestry and
adjacent grassland site in a temperate ecosystem in northern Germany. The authors utilised a custom-made closed-path gas
analyser enclosure in the LC setup. Inside the enclosure, the CO₂ mole fraction was measured with a GMP343 infrared gas
analyser, and inside the same cell, the relative humidity was measured with an HIH-4000 RH sensor. The closed-path LC EC
65 setup was compared with a conventional setup using an enclosed-path gas analyser (LI-7200, LI-COR Inc., Lincoln, NE,
USA). The LC EC CO₂ fluxes were lower compared to conventional EC by 4%–7% ($R^2 = 0.91$ – 0.95). Ramshorst et al. (2024)
concluded that LC EC had the potential to measure EC fluxes at a grassland and agroforestry system at approximately 25% of
the cost of a conventional EC system. Callejas-Rodelas et al. (2024) performed an extensive comparison of LC EC
measurements with a conventional setup above monocropping and agroforestry systems over a four-month period in 2022.
70 Again, the GMP343 sensor was used in an LC EC setup for CO₂. The authors reported satisfactory agreement between the LC
and conventional EC systems, with regression slopes of 30-min average fluxes ranging from 0.95 to 1.05 and R^2 values from
0.88 to 0.92.

The referenced studies on LC EC setups for CO₂ utilised the Vaisala GMP343 CO₂ sensor. Turbulent frequencies close to the
75 surface scale with the wind speed and are inversely proportional to measurement height; in addition, stable atmospheric
stratification favours high-frequency spectral shift. The Vaisala GMP343 sensor has a response time of approximately 1 sec.
Therefore, it is not suitable for EC application for all measurement sites and stratification conditions. In this paper, we discuss
the development of an LC gas analyser for EC CO₂ and H₂O measurements and performance characteristics of a closed-path
prototype. Measurements were conducted under agricultural field conditions and compared with simultaneous observations
80 from a commercial high-performance EC system. We report the instrument's main characteristics as well as the comparison
results obtained, aiming to assess the LC instrument's capabilities to accurately measure CO₂ balances over several months.



2 Instrumentation and methods

Development of the instrument was undertaken by Vaisala Oy in 2022 by utilizing the grant from The Finnish Research Impact Foundation that facilitated cooperation with the University of Helsinki. The aim of the study was to develop a fast-response
85 CO₂ probe, which would be cheaper than the currently commercially available ones without significant compromises in performance, and to build a concept for an easy-to-use, complete eddy covariance package. Also, field measurements were conducted to test the performance of the prototype and evaluate its characteristics under field conditions.

2.1 LC EC sensor

In order to increase the robustness of the instrument under field conditions, an enclosed-path prototype was developed. The
90 sensor utilized a thermopile detector and had internal temperature and pressure sensors capable of compensating for temperature, pressure and water vapour dilution. The enclosed path prototype had a sampling line length of 70 cm with an inlet filter and a pump capacity for a flow rate of 10-15 L min⁻¹. The power consumption of the prototype was rated from 2-3 W, with an additional 10 W power needed for pump operation. The main feature of the instrument was its built-in autocalibration capability. The auto-calibration functionality was improved several times during the field measurements period
95 and the changes had implications to sensor performance characteristics (see below).

2.2 Field measurements

The measurements reported in this study were performed at Haltiala cropland (60°16.301'N, 24°56.669'E), located in Vantaa, southern Finland, from 22 June to 16 November, 2022. The site was cultivated with oats during the measurement period. The sowing was done on 4 May and the harvest on 16 August. The measurements consisted of two separate EC setups. The EC
100 setup with Vaisala prototype analyser (further referred to as the prototype analyser/sensor or system) was located at 2.15 m height and the setup with the LI7200RS CO₂/H₂O analyser (Li-Cor Environmental, Lincoln, NE, USA) was set up at a height of 2.9 m. The Licor setup (the reference setup) used the standard 10 Hz sampling rate, whereas the prototype setup sampled 5 Hz. The flow rates for the prototype and reference systems were 10 and 12 L min⁻¹, respectively. The sampling lines in both setups were heated, with lengths of 70 cm and 91 cm for the prototype and reference setups, respectively. Both setups included
105 the Metek uSonic-3 Scientific anemometer (METEK GmbH, Germany) to measure the three wind velocity components.



Figure 1: Left: Field installation of the reference (left tower) and the prototype (right tower) eddy covariance systems at Haltiala test site. Right: The prototype setup with Metek uSonic-3 anemometer.

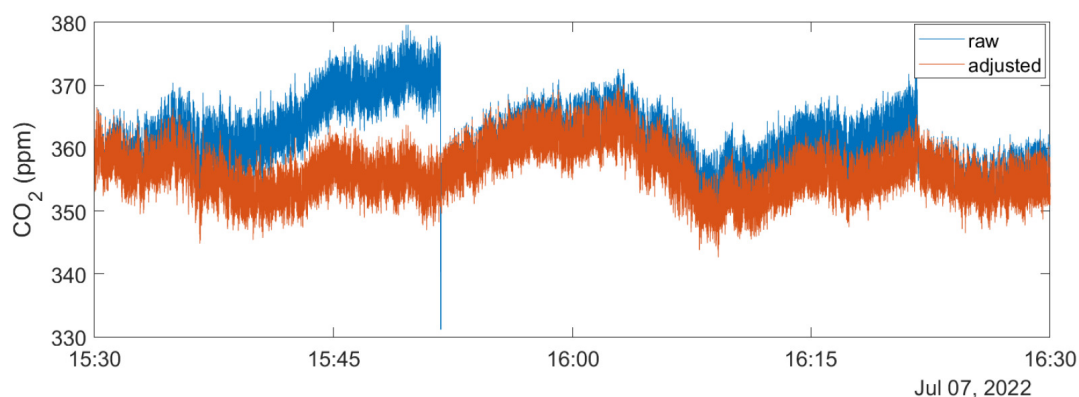
During field measurements, the sensor performance was continuously monitored, and the instrument's autocalibration
110 functionality was improved by several software updates. Initially, autocalibration was set to occur once every 30 min period. The main software update took place on 21 July 2022 around 10:00 UTC. After that, the updates took place on 25 August 2022



at 10:30-11 UTC and 30 August 2022 between 12:30-13:10 UTC. The instrument was taken to Vaisala headquarters for maintenance on 8 September 2022 and returned to the field on 20 September 2022. The instrument received two more software updates on 27 October 2022 and 31 October 2022. The maintenance breaks resulted in measurement gaps in particular in
115 September to November months, see Figs. S1, S2. The impact of software updates on system performance is discussed in the following sections.

2.3 Data processing

The software update that most significantly impacted the sensor performance took place on 21 July at around 10 am UTC. Prior to this update, the autocalibration was performed in about 30 min intervals, and the sensor output readings experienced
120 drifting, which, after periodic online calibration, resulted in signal jumps. We performed linear trend removal between the two consecutive calibrations, ensuring that the readings prior to calibration matched those after calibration (see example in Fig. 2). After the software update on 21 July, these signal jumps during calibration were removed. Thus, well-designed autocalibration functionality appeared to be a critical feature of the prototype with the thermopile detector.



125 **Figure 2: An example of turbulent CO₂ signal recorded by the prototype sensor before (raw, blue) and after calibration jump correction (adjusted, orange) prior to instrument's software update on 21 July 2022.**

We calculated the turbulent fluxes using the EddyUH version 1.8 software (Mammarella et al., 2016). The fluxes were
130 calculated for 30 min periods. Prior to flux calculation, we performed running mean high-pass filtering using a time constant of 150 sec. This was to remove potential instrumental trends in the prototype sensor signal observed before the software update on 21 July 2022. For consistency, the Licor's signal was processed the same way. Prior to flux calculation, we performed standard data processing steps available in EddyUH, such as the raw data despiking, double rotation of the coordinate system for the velocity components and time-lag correction via cross-covariance maximization. For the prototype system, the lag time
135 for the CO₂ signal varied from 0.4 to 0.8 sec with a pronounced maximum at 0.6 sec. The variation was smaller for the reference system, ranging between 0.2 and 0.4 sec, with a maximum found at 0.3 sec. Because the sampling lines were short, we did not expect the true lag time to vary, therefore, we fixed the lag times for CO₂ in further calculations. For H₂O, we observed variation in lag time with relative humidity and used such dependence in the final flux calculation. Underestimation in the low-frequency spectral range was corrected using the theoretical transfer functions (Rannik and Vesala, 1999), while the high-frequency range was corrected via experimental transfer functions (Mammarella et al., 2009) for gas fluxes and theoretical transfer functions for momentum and sensible heat flux (Moncrieff et al., 1997). The density effect of water vapour fluctuations (Webb et al., 1980) was applied to the prototype instrument's 30 min average fluxes, while for the reference sensor, the correction was not relevant because of the internal conversion of wet mole fraction to dry one.
140

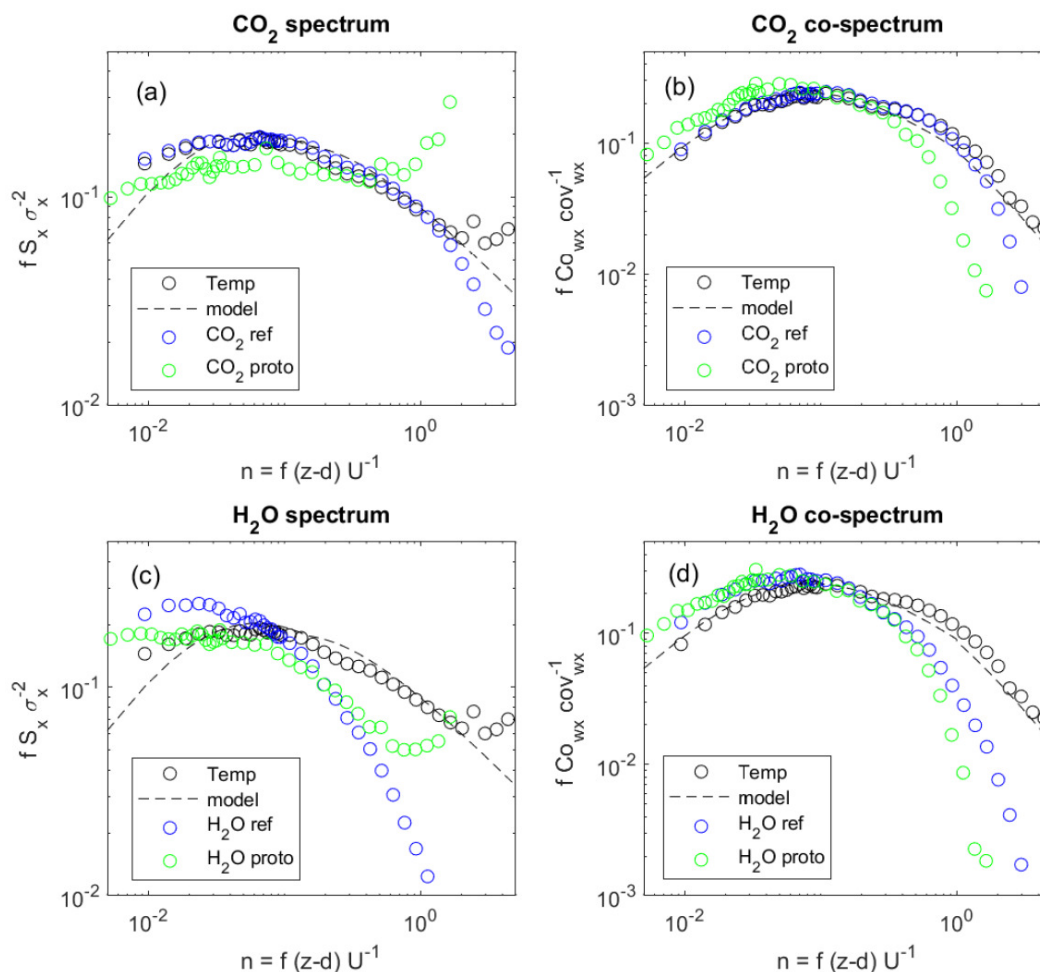


To quantify the frequency performance of the prototype system, we calculated the instrumental frequency response functions
145 using good-quality observations from daytime in June and July 2022. The response times of the instruments were obtained by
dividing the ensemble-averaged cospectrum of CO₂ by that of temperature and using least-squares fitting of the first-order
frequency response function (e.g., Peltola et al., 2021). The instrumental noise values for were estimated by using the method
described in Lenschow et al. (2000).

3 Results and discussion

150 3.1 Evaluation of system characteristics

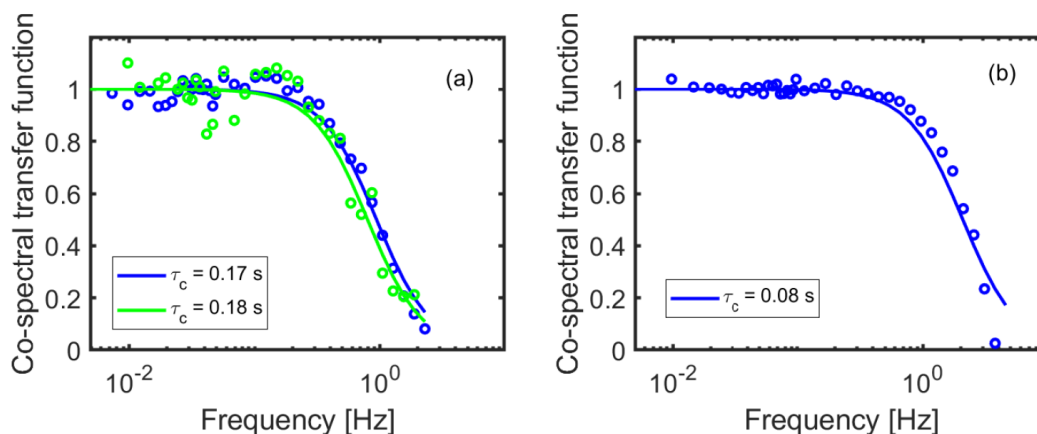
The ensemble-averaged power spectrum of the prototype system indicated the presence of noise at high frequencies in the CO₂
signal (Fig. 3a). The power spectrum of CO₂ for the reference system did not evidence any noise but rather minor damping of
the signal at high frequencies when compared to the model curve. Compared to the CO₂ spectrum, the H₂O spectrum showed
relatively less noise in the prototype sensor signal (Fig. 3c). The cospectra indicated damping of high-frequency fluctuations,
155 particularly for H₂O (Fig. 3b,d). Note that the temperature cospectrum corresponded very well to the model cospectrum.
Despite the short sampling line of the enclosed setup, damping of the H₂O signal is a common phenomenon attributable to
relative humidity effects (Fratini et al., 2012).



160 **Figure 3: Ensemble average spectra and cospectra for CO₂ (a and b) and H₂O (c and d), averaged over the June-July (till 21 July 2022) period for the reference and prototype sensors. Unstable conditions were chosen (sensible heat flux > 25 W m⁻²) with a limitation of wind speed from 2.5 to 3.5 m s⁻¹. The model curves for scalar spectra and cospectra correspond to formulations in Rannik and Vesala, 1999. Temperature spectra were obtained using the reference system sonic anemometer measurements.**

165 Using data from unstable conditions and limiting the wind speed interval for ensemble-averaging of cospectra resulted in relatively smooth curves for response time estimation (Fig. 4). The obtained result for CO₂ (first-order response time of 0.17-0.18 sec) was in good correspondence with the response time obtained for the prototype instrument in laboratory measurements (0.2 sec, not shown). The response time was very similar for both the periods before and after the software updates on 22 July 2022. A similar analysis for the reference system using the LI7200RS analyser was performed, yielding the respective response

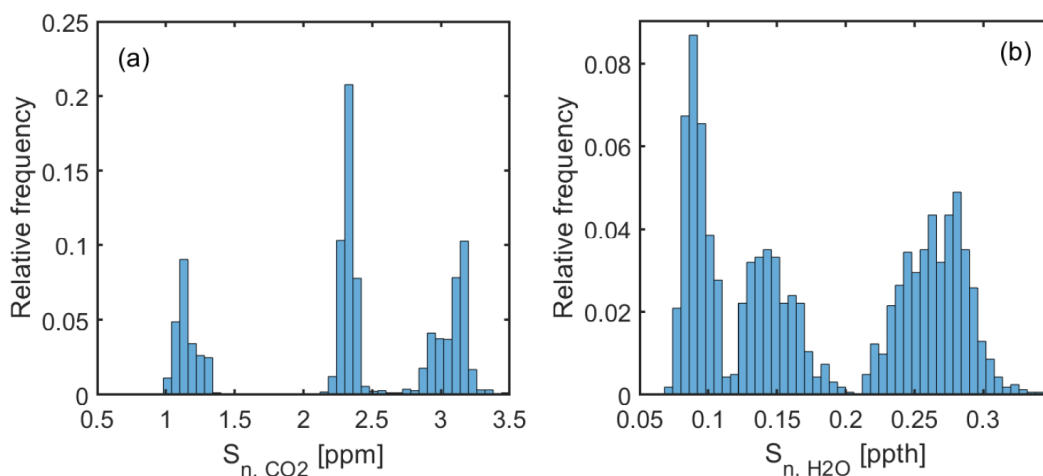
170 time of 0.08 sec.



175 **Figure 4: Frequency response functions estimated for (a) the prototype and (b) the reference systems. For transfer function estimation, unstable conditions were chosen (sensible heat flux > 25 W m⁻²) with a limitation of wind speed from 2.5 to 3.5 m s⁻¹. The period was taken from the beginning of measurements till the software update on 21 July 2022 (blue curves and symbols). For the prototype system, the response function was estimated also from 21 July (after the software update; green) till 31 July 2022.**

180 The histograms of the noise values showed three distinct peaks, corresponding to different sub-periods of measurements and caused by the changes in the instrument's signal processing after firmware upgrades (Fig. 5). Initially, the noise level for CO₂ was between 2-2.5 ppm and for H₂O 0.1-0.2 ppth. An increase in signal noise level occurred on 21 July to about 3 ppm for CO₂ and 0.2-0.3 ppth for H₂O. After the maintenance and the software update on 20 September 2022, the noise level of the signal dropped to about 1.1 ppm level for CO₂ and to 0.1 ppth for H₂O. The signal noise of CO₂ around 1 ppm is an order of magnitude larger than the noise level of the reference LI7200RS instrument (reported to be 0.08 ppm at 5 Hz for CO₂).

185 However, the noise level of 1 ppm corresponded roughly to flux random uncertainty of 5x10⁻³ ppm ms⁻¹ (approx. 0.24 μmol m⁻² s⁻¹) at 5 Hz sampling rate, assuming the averaging time 30 min and the representative value of the standard deviation of the vertical wind speed of 0.5 m s⁻¹. Thus, the flux random uncertainty due to the instrumental noise was relatively small considering the typical magnitude of flux random uncertainty due to the stochastic nature of turbulence, being in the order of 10 to 20% of the flux magnitude (Rannik et al., 2016).

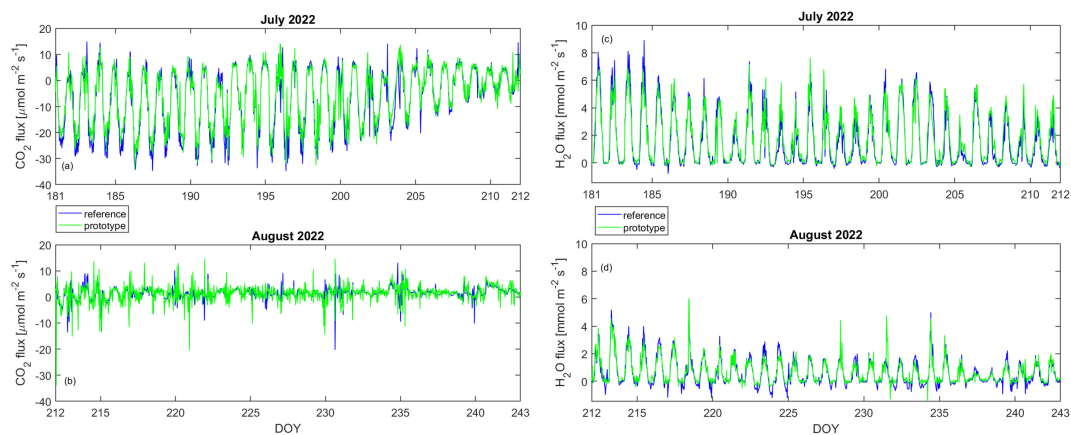


190 **Figure 5: Histograms of the instrumental noise values a) for CO₂ and b) for H₂O determined by the method of Lenschow et al. (2000) for the prototype system.**



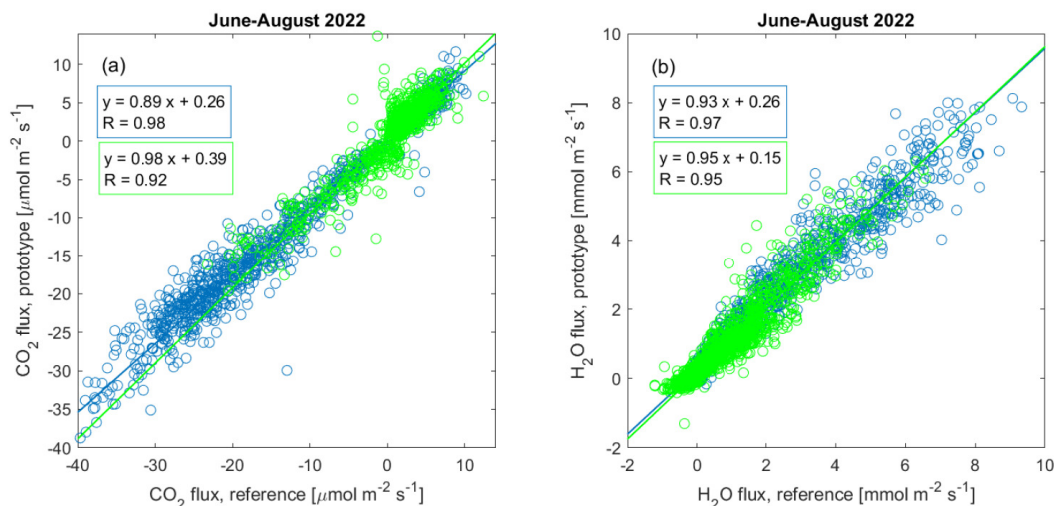
3.2 Evaluation of average fluxes

195 The CO₂ fluxes had a strong diurnal variation in July and decreased in absolute values towards the end of August (Fig. 6a,b). Significant decrease in CO₂ fluxes took place earlier than the harvest; the transition from regular diurnal pattern to relatively irregular fluxes in the end of July was related to oat senescence. In July, the CO₂ fluxes ranged from about -30 μmol m⁻² s⁻¹ during the daytime to 10 μmol m⁻² s⁻¹ at night. In August, CO₂ fluxes were highly variable with a less clear diurnal pattern compared to those in July. This applied to measurements of both systems and was attributed to variability in fluxes during oat senescence and after the harvest rather than the (random) uncertainty in the measurements. The H₂O fluxes were more regular, including the diurnal variation in August (Fig. 6c,d). The H₂O fluxes ranged from about near-zero at night to +8 mmol m⁻² s⁻¹ during the daytime in the first half of July. The daily maximum H₂O flux values decreased to about 2 mmol m⁻² s⁻¹ by the end of August.



205 **Figure 6: Time series of 30 min average fluxes measured by the prototype (green) and the reference (blue) systems for July (a – CO₂ flux, b – H₂O flux) and August (c – CO₂ flux, d – H₂O flux).**

For further analysis of potential systematic differences between the systems, we plotted the half-hour average fluxes obtained from the prototype system against the reference system values, separating the period prior to and after the software update of the prototype sensor on 21 July 2022 (Fig. 7). The slopes obtained via the orthogonal regression procedure indicated underestimation of the flux magnitude by the prototype sensor compared to the reference system. However, the underestimation was reduced after the software update, as indicated by the regression statistics (see also Fig. 8). We note that the fluxes obtained by the two systems were well correlated with high values of the coefficient of determination ($R^2 = 0.92$ - 0.98 for CO₂ fluxes and ~ 0.96 for H₂O fluxes). The random errors of the CO₂ fluxes due to noise were around 0.2 to 0.3 μmol m⁻² s⁻¹ for the prototype system (Sect. 3.1), which is much lower than the scatter in Fig. 7a. The main source of the scatter can be attributed to the random uncertainty of fluxes due to stochastic nature of turbulence because the sensors, being separated horizontally by about 5 m distance as well as vertically by 0.75 m, were not sampling exactly the same turbulence.



220

Figure 7: Comparison of 30 min average fluxes (a – CO₂, b – H₂O) of the prototype system with the reference system. The fitting parameters were obtained by using the orthogonal regression method. Blue and green colours represent the measurements (and regressions statistics in respective bounding boxes) prior to and after the software update on 21 July 2022, respectively.

225 The diurnal variation of CO₂ fluxes was notably lower from August onwards compared to June and July (Fig. 8a-e), and the difference in CO₂ fluxes between the two systems was smaller after the software update on 21 July. The magnitude of the H₂O fluxes between the systems was similar throughout the period (Fig. 8f-j). The sensible heat fluxes of the two systems were very close (Fig. 8k-o). This indicates that flux corrections for sensible heat account adequately for low-frequency underestimation that is expected to be slightly different for the two systems because of different measurement heights. In
 230 August, the H₂O fluxes were reduced and the sensible heat fluxes increased compared to July, indicating re-partitioning of the available energy after oat senescence in the end of July.

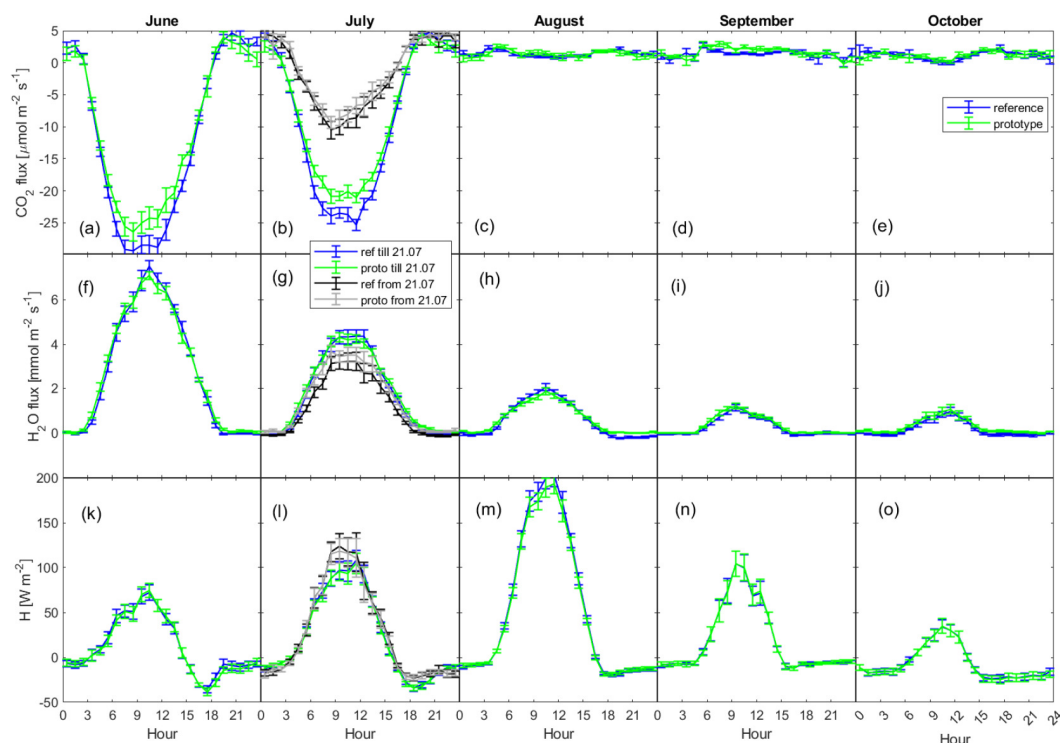
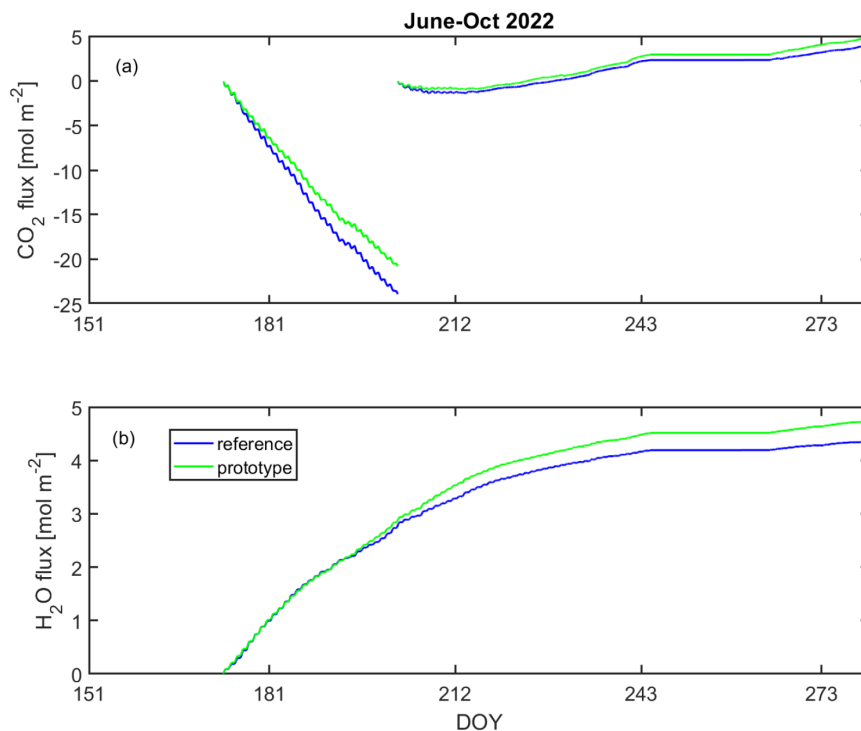


Figure 8: Monthly mean diurnal variation for CO₂ (a-e), H₂O (f-j) and sensible heat H (k-o) fluxes. In July (b, g, l), the period after the software update on 21 July 2022 is differentiated by black for the reference and grey for the prototype system.

The cumulative fluxes diverged for CO₂ prior to the software update on 21 July (Fig. 9a) by 3.1 mol m⁻² (-13%). After the update, the absolute difference was smaller. Starting from August, CO₂ fluxes were small, and from 21 July till the end of the field measurement period, the difference in cumulative flux was 0.8 mol m⁻² (+18%). Considering the small values of the cumulative fluxes (4.0 mol m⁻² for the reference system), the difference between the results from the two systems can be considered small. The software update on 21 July improved the performance of the prototype sensor, resulting in a nearly production-ready analyzer. For H₂O fluxes, the opposite was observed: until the software update, the difference between the cumulative values was small, after which the difference started to increase (Fig. 9b). The increased difference could be attributed to larger uncertainty in the high-frequency flux loss corrections at higher relative humidity conditions (for average diurnal variation of RH in each month see Fig. S3 and estimated system response time dependencies on RH see Fig. S4). Under such conditions, the overall system response is deteriorating for H₂O due to absorption/desorption of water in the sampling line. Despite determining the RH-dependent frequency response functions and applying the corrections respectively, which is a common practice (e.g. Mammarella et al., 2009), the difference in cumulative H₂O fluxes remained. The current study focused on analyzing the CO₂ sensor's performance, so its ability to measure water fluxes with high accuracy was not prioritized in this analysis. The simultaneous measurement of H₂O concentration inside the sensor's sampling cell is a prerequisite for accurate CO₂ flux measurements due to density fluctuations created by variations in water concentration (Webb et al., 1980). However, the uncertainty introduced to H₂O fluxes of the reference system by spectral attenuation due to absorption/desorption effect in the sampling line does not impact the CO₂ flux detection accuracy of the system.



255

Figure 9: Cumulative fluxes for CO₂ (a) and H₂O (b) measured by the reference (blue) and the prototype (green) systems. For CO₂, the cumulative value is reset to zero on 21 July 2022 (doy 202.4) due to a major software update. Cumulative curves were calculated over the periods when measurements from both systems were available; no gap-filling was done.

4 Summary and conclusions

260 A prototype of a LC high-response sensor was developed to measure CO₂ and H₂O concentrations, suitable for use in EC applications. We tested the enclosed-path setup in field conditions in summer and autumn 2022. The field setup included a separate reference measurement system containing commonly used instruments in scientific applications (Metek uSonic-3 Scientific sonic anemometer and Licor LI-7200 gas analyzer). The LC prototype was developed by Vaisala Oyj in cooperation with the University of Helsinki. The sensor was designed to be inexpensive, easy-to-use and with minimized maintenance
265 needs. The prototype sensor was aimed to compromise accuracy, reliability, and price. More specifically, the design was based on a thermopile detector operating at two channels for CO₂ and H₂O. The sensor was operating at 5 Hz measurement frequency and included internal temperature and pressure sensors to compensate for temperature, pressure and water vapour dilution. The prototype was equipped with an autocalibration feature for reference signal verification. The prototype analyser showed improving performance throughout the campaign, which was implemented with multiple software updates. When
270 autocalibration was applied at 30-min intervals, the sensor using the early versions of the software suffered from signal drifting and jumps after applying autocalibration. The software update, performed approximately one month after the start of the field measurements (21 July 2022), fixed the issue with signal drifting.

The instrument's response time of 0.18 sec for CO₂ allowed good accuracy of measurements with relatively small co-spectral corrections at field measurements over low vegetation. The noise level of the instrument was affected by the software changes and reached about 1 ppm for CO₂ and 0.1 pph for H₂O by the end of the campaign in November 2022. Such a noise level would imply flux random uncertainty of about 0.2 $\mu\text{mol m}^{-2} \text{s}^{-1}$ under typical observation conditions, much lower than the
275



random uncertainty due to the stochastic nature of turbulence (can be a few $\mu\text{mol m}^{-2} \text{s}^{-1}$, considering typical uncertainties from 10 to 20% of the flux magnitude, Rannik et al., 2016). The LC prototype achieved also good long-term accuracy of the CO_2 flux measurements and was capable of detecting the cumulative CO_2 flux with minimal systematic bias (after the software update on 21 July).

The achieved sensor performance showed high potential in balancing the substantially lower target price of currently commercially available instruments with the measurement accuracy. However, a deeper market analysis was carried out by Vaisala, and subsequently, the market in 2022 was not big enough for Vaisala's investments. As a result, Vaisala froze further development and production of the sensor.

Author contribution: All co-authors were part of the project team planning the instruments design and field measurements. Pirkko Väkimies and Hilikka Heiskari-Tuohiniemi were leading the design and building of the prototype at Vaisala; Mika Korkiakoski performed field measurements and analysis of results during the project. Üllar Rannik performed final analysis and prepared the manuscript with contributions from all co-authors.

Acknowledgements: Funding by the Finnish Research Impact Foundation (project "Breathing of biosphere – Industrialization of easy-to-use carbon dioxide exchange measurements") and ICOS Finland by University of Helsinki are acknowledged.

References

- Baldocchi, D.D.: How eddy covariance flux measurements have contributed to our understanding of Global Change Biology, *Glob Change Biol.* 26, 242-260, 2019.
- Callejas-Rodelas, J. Á., Knohl, A., van Ramshorst, J., Mammarella, I., Markwitz, I.: Comparison between lower-cost and conventional eddy covariance setups for CO_2 and evapotranspiration measurements above monocropping and agroforestry systems, *Agric. Forest Meteorol.*, 354, <https://doi.org/10.1016/j.agrformet.2024.110086>, 2024.
- Cunliffe, A. M., Boschetti, F., Clement, R., Sitch, S., Anderson, K., Duman, T.: Strong correspondence in evapotranspiration and carbon dioxide fluxes between different eddy covariance systems enables quantification of landscape heterogeneity in dryland fluxes, *J. Geophys. Res.: Biogeosciences*, 127, e2021JG006240, <https://doi.org/10.1029/2021JG006240>, 2022.
- Fratini, G., Ibrom, A., Arriga, N., Burba, G., Papale, D.: Relative humidity effects on water vapour fluxes measured with closed-path eddy-covariance systems with short sampling lines, *Agric. Forest Meteorol.*, 165, 53-63, <https://doi.org/10.1016/j.agrformet.2012.05.018>, 2012.
- Hill, T., Chocholek, M., and Clement, R.: The case for increasing the statistical power of eddy covariance ecosystem studies: why, where and how?, *Glob. Change Biol.*, 23, 2154–2165, <https://doi.org/10.1111/gcb.13547>, 2017.
- Lenschow, D., Wulfmeyer, V., and Senff, C.: Measuring second through fourth-order moments in noisy data, *J. Atmos. Ocean. Tech.*, 17, 1330–1347, 2000.
- Mammarella, I., Launiainen, S., Gronholm, T., Keronen, P., Pumpanen, J., Rannik, Ü., and Vesala, T.: Relative Humidity Effect on the High-Frequency Attenuation of Water Vapor Flux Measured by a Closed-Path Eddy Covariance System, *Journal of Atmospheric and Oceanic Technology*, 26, 1856-1866, 2009.
- Mammarella, I., Peltola, O., Nordbo, A., Järvi, L., and Rannik, Ü.: Quantifying the uncertainty of eddy covariance fluxes due to the use of different software packages and combinations of processing steps in two contrasting ecosystems, *Atmos. Meas. Tech.*, 745 9, 4915–4933, 2016.



- Markwitz, C. And Siebicke, L.: Low-cost eddy covariance: a case study of evapotranspiration over agroforestry in Germany. *Atmos. Meas. Tech.*, 12, 4677–4696, <https://doi.org/10.5194/amt-12-4677-2019>, 2019.
- 320 Moncrieff, J., Massheder, J. M., de Bruin, H., Elbers, J., Friborg, T., Heusinkveld, B., Kabat, P., Scott, S., Soegaard, H., and Verhoef, A.: A system to measure surface fluxes of momentum, sensible heat, water vapour and carbon dioxide, *J.Hydrol.*, 188-189, 589-611, 1997.
- Peltola, O., Aslan, T., Ibrom, A., Nemitz, E., Rannik, Ü., and Mammarella, I.: The high-frequency response correction of eddy covariance fluxes – Part I: An experimental approach and its interdependence with the time-lag estimation, *Atmos. Meas. Tech.*, 14, 5071–5088, <https://doi.org/10.5194/amt-14-5071-2021>, 2021.
- 325 Rannik, Ü., Peltola, O., and Mammarella, I.: Random uncertainties of flux measurements by the eddy covariance technique, *Atmos. Meas. Tech.*, 9, 5163–5181, doi:10.5194/amt-9-5163-2016, 2016.
- Rannik, Ü., and Vesala, T.: Autoregressive filtering versus linear detrending in estimation of fluxes by the eddy covariance method. *Boundary-Layer Meteorol.*, 91, 259-280, 1999.
- 330 Romppanen, S.: The LULUCF Regulation: the new role of land and forests in the EU climate and policy framework. *Journal of Energy & Natural Resources Law* 38(3), 1-27. DOI:10.1080/02646811.2020.1756622, 2020.
- van Ramshorst, J.G.V., Knohl, A., Callejas-Rodelas, J. Á., Clement, R., Hill, T.C., Siebicke, L., and Markwitz, C.: Lower-cost eddy covariance for CO₂ and H₂O fluxes over grassland and agroforestry, *Atmos. Meas. Tech.*, 17, 6047–6071. <https://doi.org/10.5194/amt-17-6047-2024>, 2024.
- 335 Wang, K., Huang, L., Zhang, J., Zhen, X., Shi, L., Lin, T.-J., Zheng, X., Wang, Y.: Measuring Turbulent Water Vapor Fluxes using a Tunable Diode Laser-Based Open-Path Gas Analyzer, *Water*, 16, 307, <https://doi.org/10.3390/w16020307>, 2024.
- Webb, E. K., Pearman, G. I., and Leuning, R.: Correction of flux measurements for density effects due to heat and water-vapor transfer. *Quarterly Journal of the Royal Meteorological Society*, 106(447), 85-100. PT: J; NR:34; TC: 1213; J9: Quart. *J. Roy. Meteorol. Soc.*, JD792, UT:ISI:A1980JD79200007, 1980.

340